Investigating the yield of H_2O and H_2 from methane oxidation in the stratosphere

Franziska Frank[1], Patrick Jöckel[1], Sergey Gromov[2,3], and Martin Dameris[1]

[1]Deutsches Zentrum für Luft- und Raumfahrt (DLR), Institut für Physik der Atmosphäre, Oberpfaffenhofen, Germany
[2]Max-Planck-Institute for Chemistry, Air Chemistry Departement, Mainz, Germany
[3]Institute of Global Climate and Ecology Roshydromet & RAS (IGCE), Moscow, Russia

Correspondence to: Franziska Frank (franziska.frank@dlr.de)

Abstract. An important driver of climate change is stratospheric water vapour (SWV), which in turn is influenced by the oxidation of atmospheric methane (CH_4). In order to parameterize the production of water vapour (H_2O) from CH_4 oxidation, it is often assumed that the oxidation of one CH_4 molecule yields exactly two molecules of H_2O. However, this assumption is based on an early study, which also gives evidence, that this is not true at all altitudes.

5 In the current study we re-evaluate this assumption with a comprehensive systematic analysis using a state-of-the art Chemistry-Climate model (CCM), namely the ECHAM/MESSy Atmospheric Chemistry (EMAC) model, and present three approaches to investigate the yield of H_2O and hydrogen gas (H_2) from CH_4 oxidation. We thereby make use of Module Efficiently Calculating the Chemistry of the Atmosphere (MECCA) in a box model and global model configuration. Furthermore, we use the kinetic chemistry tagging technique (MECCA-TAG) to investigate the chemical pathways between CH_4, H_2O and H_2, by being able to distinguish hydrogen atoms stemming from CH_4 and other sources.

10 We apply three approaches, which all agree that assuming a yield of 2 overestimates the production of H_2O in the lower stratosphere (calculated as 1.5–1.7). Additionally, transport and subsequent photochemical processing of longer-lived intermediates raise the local yield values in the upper stratosphere and lower mesosphere above 2 (maximum > 2.2). In the middle and upper mesosphere, the influence of loss and recycling of H_2O increases, making it a crucial factor in the parameterization of the yield of H_2O from CH_4 oxidation. An additional sensitivity study with the Chemistry As A Boxmodel Application (CAABA) shows a dependence of the yield on the hydroxyl radical (OH) abundance. No significant temperature dependence is found. We focus representatively on the tropical zone between 23° S-23° N. It is found in the global approach that presented results are mostly valid for mid latitudes as well. During the polar night the method is not applicable.

Our conclusions question the use of a constant yield of H_2O from CH_4 oxidation in climate modeling and encourage to apply
20 comprehensive parameterizations that follow the vertical profiles of the H_2O yield derived here and take the chemical H_2O loss into account.

1 Introduction

It is beyond question that water vapour (H_2O) is an important greenhouse gas (GHG). The current study focuses on stratospheric water vapour (SWV), which is by itself an influential driver of climate change. SWV, for example, induces a reduction of

stratospheric ozone concentration (Stenke and Grewe, 2005; Revell et al., 2016), cools the stratosphere (Revell et al., 2012; Forster and Shine, 1999; Maycock et al., 2014) and produces a positive radiative forcing (Solomon et al., 2010). Changes in SWV are mainly driven by troposphere-stratosphere exchange (e. g. through deep convection in the tropics (Fueglistaler and Haynes, 2005)). However, there is also a chemical contribution to SWV, mostly by oxidation of methane (CH_4) and

5   hydrogen gas (H_2). These gases are still abundant above the tropopause to act as significant in-situ photochemical sources of H_2O. Besides H_2O, CH_4 is a powerful GHG as well, with a 34 times higher climate effect than an equivalent amount of carbon dioxide (CO_2) on a time horizon of 100 years (IPCC, 2013). It also introduces secondary climate effects through the additional SWV. The strong linkage of CH_4 and SWV represents a decisive factor of the net climate effect of CH_4. Enhanced CH_4 concentrations are likely expected in the future Earth's atmosphere and can impact the otherwise rather dry stratosphere

10 substantially (Rohs et al., 2006).

Nevertheless, to account for the contribution of CH_4 to SWV, in current climate modeling it is common either to use a Chemistry-Climate model (CCM) with a complex chemistry set up, which puts high demands on computational resources, or a General Circulation model (GCM) or Chemical Transport model (CTM) with – if at all – a parameterization of the chemical sources of SWV. A parameterization of the chemical feedback onto SWV requires to estimate the yield of H_2O from CH_4

15 oxidation, which is defined as the production of H_2O per oxidized CH_4 molecule. A common simple assumption of the yield of H_2O from CH_4 oxidation is that one oxidized CH_4 molecule produces two H_2O molecules in the stratosphere. This simple parameterization is based on a first estimation of the H_2O yield from CH_4 oxidation, using a simplified methane chemistry without chlorine in a two dimensional photochemistry model (le Texier et al., 1988).

This is a widely accepted approximation (Myhre et al., 2007; Stowasser et al., 1999) and is also affirmed by aircraft ob-

20 servations, which state that $2 \cdot [CH_4] + [H_2O]$ (also named as the total stratospheric hydrogen budget) is fairly constant in the stratosphere being 6.8-7.6 ppmv (Hurst et al., 1999; Rahn et al., 2003; Dessler et al., 1994; Stowasser et al., 1999). Although this suggests that all atomic hydrogen (H) from CH_4 oxidation reaches H_2O, it must be noted that the referenced observation studies do not distinguish, whether the H in H_2O comes from CH_4 or from H_2, which also originates from the troposphere. Thus, calculations based on observed mixing ratios show a net production of H_2O only, but not the yield of H_2O specifically

25 from CH_4 oxidation (Hurst et al., 1999). Furthermore, H_2 mixing ratios, when measured as well, show an almost absent vertical gradient, which can be explained by the supposition that the H_2 sink is in photochemical equilibrium with its production from CH_4 oxidation. Hence, all additional H_2 by CH_4 is leveled by the oxidation of H_2 and balances the $2 \cdot [CH_4] + [H_2O]$ and H_2 content in the stratosphere (Rahn et al., 2003). Nevertheless, Hurst et al. (1999) took the weak anti-correlation of H_2 and CH_4 into account and calculated a net production of H_2O over loss of CH_4 of 1.973 $\pm$0.003, differing from the assumed value of

30 2, which would be the case if all H goes into H_2O. By analysing satellite based measurements Wrotny et al. (2010) derived a production of H_2O over loss of CH_4 ratio of 2.0–3.7 in the upper stratosphere between 1.0–4.6 hPa, which is clearly ≥ 2.

Still, for reasons of simplification, several GCMs use the approximation that the yield of H_2O from CH_4 oxidation is exactly two (Monge-Sanz et al., 2013; ECMWF, 2007; Austin et al., 2007; Oman et al., 2008; Boville et al., 2001; Mote, 1995; Eichinger et al., 2015). In the ECHAM/MESSy Atmospheric Chemistry (EMAC) model (Jöckel et al., 2010), for example,

35 explicitly configured in a CTM-like set-up without interactive chemistry, the production of SWV from CH_4 oxidation is calcu-

lated in a simplified way using a specifically introduced CH_4 tracer (by applying the CH4 submodel) according to:

$$\frac{d}{dt}[H_2O] = -\gamma_{H_2O} \cdot \frac{d}{dt}[CH_4] \tag{1}$$

with $\gamma_{H_2O} = 2$ as the yield of H_2O. Note, that if one wants to apply such a parameterization, one must specifically be aware not to mix yield of H_2O from the oxidation of CH_4 (γ_{H_2O}) with the yield from the oxidation of H_2, originating from the troposphere.

However, this approximation first and foremost neglects the chemical loss of H_2O (mostly by reaction with excited oxygen ($O(^1D)$) and by photolysis). Using this parameterization, SWV is solely added and not removed by chemistry. Moreover, the results of le Texier et al. (1988) also suggest that the yield of H_2O from CH_4 oxidation is not exactly two, accounting for the part of H diverted into H_2 production and that the share of H_2 increases at higher altitudes. Therefore, following the results of le Texier et al. (1988) precisely, we would generate a certain bias by using a yield of 2 in Eq. (1), especially at higher altitudes, where $2 \cdot [CH_4] + [H_2O]$ approx. const. does not hold anymore. In the mesosphere, for example, the loss of H_2O becomes increasingly relevant, shifting the balance between H_2O and H_2 towards the latter. Furthermore, the net production calculated by Hurst et al. (1999) and the yield of le Texier et al. (1988) also do not agree well in the lower stratosphere, which can indeed be explained by the indistinguishable inputs from H_2 and CH_4 oxidation in observations as stated before. Yet, this does also indicate that the yield from CH_4 oxidation itself must be even lower than suggested by the net production, which is calculated based on observations. It is, therefore, questionable, if the assumption of $\gamma_{H_2O} = 2$ for the CH_4 oxidation is indeed applicable.

In this study we re-evaluate the findings of le Texier et al. (1988) with multiple approaches using a modern CCM with a complex state-of-the-art chemistry mechanism. Our goal is to assess the currently used assumption of the constant yield as in Eq. 1 with $\gamma_{H_2O} = 2$ and investigate, if a parameterization solely based on CH_4 is sufficient to reproduce the chemical yield of H_2O from CH_4 oxidation. As an additional remark, it should be noted that difficulties with yield estimates can be expected especially in the stratosphere, as it is vertically not as well mixed as the turbulent troposphere.

We show three approaches to determine the yield of H_2O from CH_4 oxidation. The first two approaches use the kinetic chemistry tagging technique (MECCA-TAG, Gromov et al. (2010)), either (1) in a box model set-up with the Chemistry As A Boxmodel Application (CAABA, Sander et al. (2011a)) and (2) in a global simulation, with the EMAC (Jöckel et al., 2010) model. For the third approach (3) we again use the model results of a global simulation with EMAC. This approach relies on the assumption that the hydrogen budget in the stratosphere is conserved, mostly consisting of fractions of H, H_2, H_2O and CH_4.

We apply MECCA-TAG (Gromov et al., 2010) in all approaches to run a comprehensive chemistry setup, while being able to track the production of H_2O originating explicitly from CH_4 oxidation. A conceptionally different approach would be the extended Crutzen's sequential method used by Johnston and Kinnison (1998) to estimate the gross ozone loss by CH_4. The study of Johnston and Kinnison (1998) is an additional example for estimating a yield from CH_4 oxidation, although it focuses on CH_4 impacts on ozone (O_3) instead of H_2O. By applying MECCA-TAG, however, it is not necessary to explicitly write down the chemical net reactions as this is done in the extended Crutzen's sequential method.

The paper is structured as follows: In section 2 we present the methods and theoretical background of our studies, followed by the results in section 3. Section 4 comprises a detailed discussion and section 5 summarizes the findings and gives an outlook for further studies.

2   Methods

2.1   The model set-up

2.1.1   EMAC

The applied global chemistry climate model is EMAC, which is a state-of-the art numerical chemistry and climate simulation system that includes sub-models describing tropospheric and middle atmosphere processes and their interaction with oceans, land and human influences (Jöckel et al., 2010). It uses the second version of the Modular Earth Submodel System (MESSy) to link multi-institutional computer codes. The core atmospheric model is the 5th generation European Centre Hamburg general circulation model (ECHAM5) (Roeckner et al., 2006). For the global simulations in the present study we applied EMAC (ECHAM5 version 5.3.02, MESSy version 2.53.0) in the T42L90MA-resolution, i.e. with a spherical truncation of T42 (corresponding to a quadratic Gaussian grid of approx. 2.8 by 2.8 degrees in latitude and longitude) with 90 vertical hybrid pressure levels up to 0.01 hPa. The applied model setup comprises particularly the submodels MECCA (Module Efficiently Calculating the Chemistry of the Atmosphere) (Sander et al., 2005) and MECCA-TAG (kinetic chemistry tagging technique) (Gromov et al., 2010).

The MECCA represents the chemical core of EMAC. The applied chemistry is based on a chemical mechanism, which, for example, was already used for the base simulations in the Earth System Chemistry integrated Modelling (ESCiMo) project (Jöckel et al., 2016). The mechanism is extended to resolve specific intermediates in the $CH_4 \rightarrow H_2O$ reaction chain (e.g. methyl (CH_3) and methoxy radical (CH_3O)), resulting in slightly more comprehensive chemical kinetics. The full chemical mechanism is part of the supplement.

2.1.2   The kinetic tagging technique MECCA-TAG

MECCA-TAG (Gromov et al., 2010) enables the user to tag certain elements, without modifying the underlying standard chemical mechanism. It can either be applied for simulating isotopologues of selected trace gases or used to investigate elemental exchange between the species of interest. For example, a model study was carried out with focus on the carbon and oxygen isotope composition of carbon monoxide (CO) (Gromov et al., 2010).

In the current study we use the tagging technique (in the so called fractional mode) to investigate the pathways of H atom transfer from the source CH_4 to H_2O via all simulated intermediates. In order to do so, we create counterparts of the species of interest (e.g., those containing H) in an isolated doubled set of studied reactions (e.g., CH_4 oxidation chemistry) in the same chemical mechanism simulated. By doing so, we are able to quantify the fraction of molecules (hence their H content)

stemming from CH_4 oxidation only, as well as their production and loss rates, which are used for the yield calculations. Furthermore, we improve the latter by quantifying the H, which is recycled in the given reactions.

In this particular case, we count the H_2O molecules created from CH_4 oxidation pathways and are able to distinguish the H from CH_4 from the H of other sources (H_2, non-methane hydrocarbons (NMHCs), hydrochlorofluorocarbons (HCFCs), etc.). More specifically, we track the H atoms, which all have in common that their source is only CH_4. These H atoms can temporarily be part of H_2, but we are not counting oxidation of H_2, which is produced in the troposphere and transported into the stratosphere. However, we are accounting for hydrogen, which has been part of CH_4 produced H_2O, and which becomes recycled after depletion of H_2O. Hence, that part of CH_4 produced H_2O, which breaks down to other HOx (hydroxyl radical (OH)+hydroperoxyl (HO_2)) compounds (and subsequently produces H_2O again) is counted separately. Overall, such an approach is the "online" approximation of the technique used by Lehmann (2004) and helps to avoid double-counting issues in yield derivation. Ultimately, we are able to quantify the fraction of H atoms populating the species of the complete ($CH_4 \rightarrow H_2O/H_2 \leftrightarrow HO_x$)-cycle, including their fractions recycled via H_2O.

2.1.3 CAABA

For the photochemical box model studies we use the Chemistry As A Boxmodel Application (CAABA) in model version 3.0 (Sander et al., 2011a). CAABA equipped with MECCA (CAABA/MECCA) provides an atmospheric chemistry box model, simulating single air parcels with the chemical mechanism identical to that used in EMAC. CAABA/MECCA is, moreover, using the MESSy interface to attach certain submodels to the box model system. The used submodels in the current study, in addition to MECCA, are SEMIDEP (applies deposition fluxes) and JVAL (calculates photolysis rates) (Sander et al., 2014).

CAABA simulates one box at one pressure and temperature specific for a given latitude and altitude in the atmosphere. To derive a pseudo vertical profile of the yield, 35 independent boxes superimposed upon each other at the equator are simulated with prescribed conditions following a standard atmosphere profile ((NOAA/NASA, 1976) accessed via https://www.digitaldutch.com/atmoscalc/ (digital dutch, 1999)). The equatorial region is chosen for mainly two reasons: (1) the equatorial region is in terms of photochemistry most active and (2) we avoid the inactive photochemistry during the polar night. Since the boxes represent different temperature and pressure levels and therefore distinct chemical regimes throughout the middle atmosphere, it is possible to illustrate the vertical dependence of the yield.

Note that the purpose of the box model simulation is to demonstrate the steady state conditions expected at different altitudes. In order to do so, we mimic the effect of vertical transport between the boxes by prescribing the vertical distribution of the relevant species concentrations for:

1. CH_4 and all species acting as in-situ sources of H (primarily NMHCs and HCFCs), which are not produced in the chemical mechanism,

2. long-lived substances, such as ammonia (NH_3) and nitrous oxide (N_2O),

3. N_2 and O_2, whose mixing ratios are virtually constant throughout the considered altitude range,

4. nitrogen oxide (NO) and O(^{1}D), to constrain the HOx-NOx-cycle to the given initial state (the family NOx consists of NO and nitrogen dioxide (NO$_2$)),

5. SO$_2$, Cl and Br, for the same reason as in 4. with respect to ClOx (Cl + ClO), BrOx (Br + BrO) and sulfate compounds,

6. H$_2$O and H$_2$ mixing ratios and therefore serving as a H sink for the limitless influx of H via the fixed source species (indicated in 1.).

Other species, particularly the OH and HO$_2$, are unconstrained in the simulations unless otherwise noted. All initial mixing ratios of the chemical species are taken from a climatology over the years 2000–2010 of the RC1SD-base-10 EMAC simulation of the ESCiMo project (Jöckel et al., 2016). This simulation is carried out at T42L90MA resolution with specified dynamics, hence a Newtonian relaxation is performed with respect to meteorological reference data (ERA-Interim reanalysis data from ECMWF (Dee et al., 2011) to be more precise) concerning the prognostic variables divergence, vorticity, temperature and (logarithm of) surface pressure.

Because a priori fractions of H from CH$_4$ (or tagged H) in the species of the chemical mechanism are not known, all tagged species are initialized with zero. The simulation of every box is run for 200 years to make sure that all tagged species have filled up to a steady state.

2.2 Calculation of the chemical H$_2$O yield from CH$_4$ oxidation

A straight forward definition of the direct yield is the ratio of the production of H$_2$O molecules by the loss of CH$_4$, as depicted in Eq. (2).

$$\gamma_{H_2O}^{direct}(CH_4) = \frac{\mathbf{P}_{H_2O}^I}{\mathbf{L}_{CH_4}} \tag{2}$$

with variables listed in Table 1. The γ_{H_2O} represents the units of molecule H$_2$O per molecule CH$_4$ (i.e. [molecule/molecule]) and is displayed dimensionless throughout this work.

The loss of CH$_4$ ($\mathbf{L}_{CH_4}$) in MECCA includes the reactions with OH, O(^{1}D) and Cl, as well as photolysis (see Reactions (R1) - (R6)).
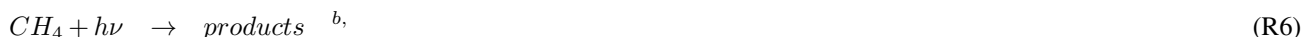
$$
\begin{aligned}
CH_4 + O(^1D) &\rightarrow CH_3 + OH & \text{(R1)}\\
&\rightarrow CH_3O + H & \text{(R2)}\\
&\rightarrow CH_2O + H_2 \quad {}^{a,} & \text{(R3)}\\
CH_4 + OH &\rightarrow CH_3 + H_2O \quad {}^{a,} & \text{(R4)}\\
CH_4 + Cl &\rightarrow HCl + CH_3 \quad {}^{a,} & \text{(R5)}\\
CH_4 + h\nu &\rightarrow products \quad {}^{b,} & \text{(R6)}
\end{aligned}
$$

with reaction rates of a, from Sander et al. (2011b) and photolysis rate of b, calculated by JVAL (Sander et al., 2014).

Table 1. Variable names as used in Equations 2, 3 and 4.

name	description
$\mathbf{L}_{CH_4}$	loss of CH_4 molecules
$\mathbf{P}^{I}_{H_2O/H_2}$	direct production of H_2O/H_2 by
	H from CH_4
$\mathbf{L}^{I}_{H_2O/H_2}$	loss of directly produced H_2O/H_2
$\mathbf{P}^{II}_{H_2O/H_2}$	production of recycled H_2O/H_2,
	hence the H already has been part
	of a H_2O/H_2 produced by CH_4
$\mathbf{L}^{II}_{H_2O/H_2}$	loss of recycled H_2O/H_2
μ_{H_2O/H_2}	lost H_2O/H_2 during the recycling

Following these reactions, H atoms from CH_4 are distributed among intermediates (not shown) and eventually reach H_2O. Produced H_2O reacts further and gets removed, by reactions (R7) and (R9).

$$H_2O + O(^1D) \quad \rightarrow \quad 2OH \qquad^{a,} \tag{R7}$$

$$SO_2 + OH + O_2 + H_2O \quad \rightarrow \quad H_2SO_4 + HO_2 \qquad^{a,} \tag{R8}$$

$$H_2O + h\nu \quad \rightarrow \quad H + OH \qquad^{b,} \tag{R9}$$

with reaction rates of a, from Sander et al. (2011b) and photolysis rate of b, calculated by JVAL (Sander et al., 2014).

In consecutive reactions H is again recycled into H_2O. The direct yield calculated by Eq. (2) represents the H_2O, which is produced in the chemical mechanism and directly emerges from CH_4 oxidation. However, this is not the additional H_2O of the whole chemical process. It also cannot be used in a simplified set-up for the methane chemistry and the production of SWV parameterized as by Eq. (1), because no chemical depletion of water is considered. Hence, we suggest to define the effective yield of H_2O, which takes into account that water is recycled in consecutive reactions and that recycled water is again destroyed. The process is sketched in Fig. 1. During this recycling process, some H is converted to species other than H_2O, filling up to a steady state or leaving the HOx-cycle once and for all. The effective yield is therefore always equal to or smaller than the direct yield in a closed system.

We define the effective yield of H_2O in this study as in Eq. (3), with μ accounting for the lost H_2O, due to subsequent loss and recycling of H_2O molecules:

$$\gamma^{eff}_{H_2O}(CH_4) = \frac{\mathbf{P}^{I}_{H_2O} - \mu_{H_2O}}{\mathbf{L}_{CH_4}} \quad \text{with} \quad \mu_{H_2O} = \mathbf{L}^{I}_{H_2O} + \mathbf{L}^{II}_{H_2O} - \mathbf{P}^{II}_{H_2O} \tag{3}$$

Variables are listed in Table 1.

Exemplarily, the components of the effective yield of H_2O of Eq. (3) are plotted separately in Fig. 2 as a vertical profile for the experiment Ref, which will be introduced in more detail in Section 3.1.2. These profiles indicate that loss of CH_4 and production of H_2O minimize around the tropopause and maximize close to the stratopause. The maximum of the primary loss
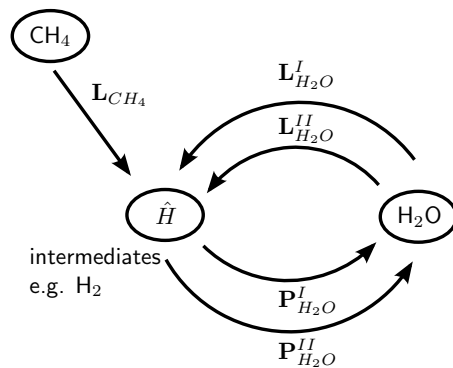
Figure 1. Sketch on the production and recycling of H_2O. The arrows of L_{CH_4} and $P^I_{H_2O}$ are indicating the direct yield and all arrows together the effective yield.
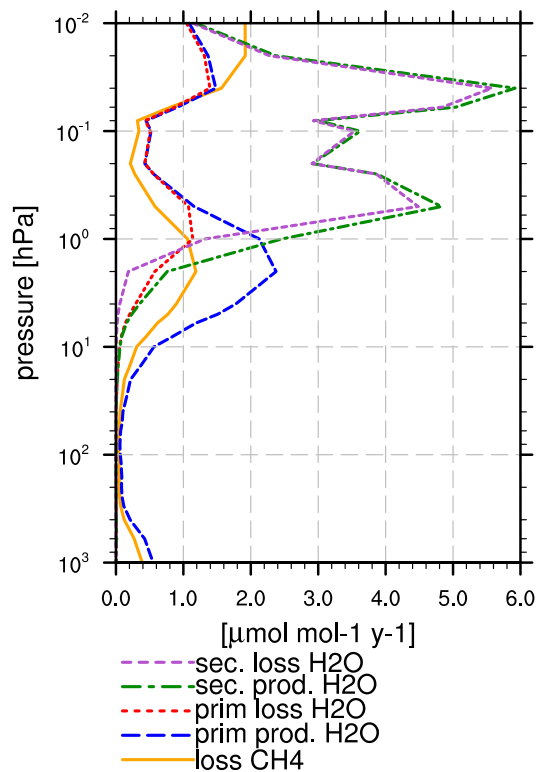
Figure 2. Separate loss of CH_4 and primary and secondary loss and production of H_2O from box model simulation Ref.

of H_2O in the stratosphere is slightly shifted vertically. Above the stratopause, the recycling of H_2O becomes more important. This is indicated by increased secondary loss and production of H_2O and is further reflected by the reduced effective yield in the mesosphere.

Due to the implementation of the tagging technique, counting of recycled H (as described in section 2.1.2) can only be applied with respect to one species at a time. Hence, the effective yield can only be calculated either for H_2O or H_2 in the same simulation. Similar to that for H_2O, recycling of H_2 is calculated in the chemical mechanism, that is, the recycled H is counted as soon as it is leaving H_2. The corresponding formula for H_2 is derived similarly to Eq. (3) and reads as follows:

$$\gamma_{H_2}^{eff}(CH_4) = \frac{\mathbf{P}_{H_2}^I - \mu_{H_2}}{\mathbf{L}_{CH_4}} \quad \text{with} \quad \mu_{H_2} = \mathbf{L}_{H_2}^I + \mathbf{L}_{H_2}^{II} - \mathbf{P}_{H_2}^{II} \tag{4}$$

Direct and effective yield are equal, as long as the loss of H_2O is negligible or the recycling is lossless.

The chemical conversion from CH_4 to H_2O follows some intermediate reactions. Hence, the loss of CH_4 and the eventual production of H_2O do not occur simultaneously. Furthermore, in reality, chemistry undergoes diurnal variations. The major changes occur during daylight. At night, virtually no photo-sensitive chemistry takes place, which results in very low OH concentrations. This reduces CH_4 loss and H_2O production to a nighttime-low. A diurnal average smoothes the difference between day and night to a representative value. This is based on the assumption that the system is in a quasi-steady-state. A quasi-steady-state implies that equal integral production and loss are simulated throughout a given time interval, e.g. a day, a month or a year. Monthly γ_{H_2O} averages, as presented in this study, which average over the simulated diurnal cycle, are sufficient for the application of a simplified CH_4 loss/H_2O production rates calculation with prescribed monthly varying OH distributions.

For these reasons, we apply in our analysis Eq. (3) to annual averages of the production and sink terms simulated in the boxes representing conditions typical for the tropics, where in addition seasonal variations are negligible. In the global simulations with EMAC we calculate an average over zonally averaged tropical bands.

In the following we compare the direct and effective yields of H_2O and H_2 from CH_4 oxidation obtained in simulations with the box model and EMAC.

3 Results

3.1 Box model approach

3.1.1 Simulation with unrestrained oxidation capacity

The direct and the effective yield of H_2O from CH_4 oxidation of the box model approach (i.e. simulation Exp1), calculated as indicated in Eq. (2) and Eq. (3) respectively, are shown as a pseudo vertical profile in Fig. 3 by 35 vertically stacked boxes following the standard atmosphere at the equator. The shown results comprise also boxes on tropospheric levels. However, since the physical water cycle (e.g. evaporation, clouds) exceeds the influence of the CH_4 oxidation onto H_2O, the kinetic
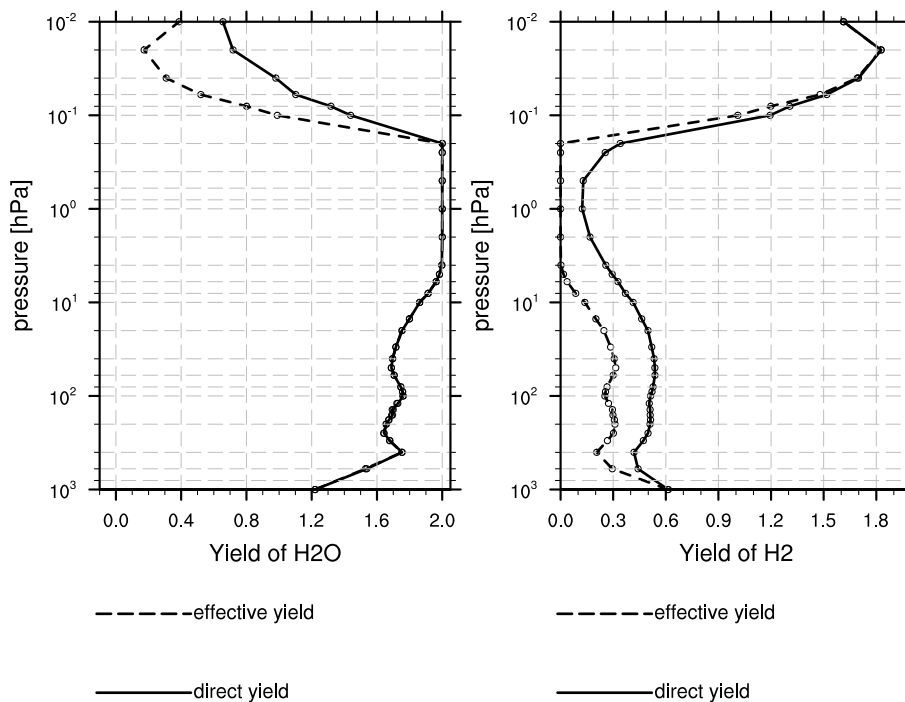
Figure 3. The pseudo vertical profile shows the H_2O yield (left) and H_2 yield (right), calculated by the box model approach. The solid line represents the direct yield, the dashed line represents the effective yield and circles indicate the pressure levels of the model boxes.

production of H_2O is irrelevant in the troposphere. All values below the tropopause level (approximately 100 hPa in the tropics) are therefore not part of the analysis presented in this work.

The direct yield in Fig. 3 (left) is 1.7 around the tropopause and increases monotonically up to 2 at 4 hPa. It remains constant until 0.2 hPa, where it starts to decrease monotonically down to about 0.65 at the uppermost layer. In the mesosphere the loss
5 of H_2O especially via Reactions (R7) and (R9) increases (also evident in Fig. 2).

The direct and the effective yields do not differ significantly for water vapor throughout the stratosphere and most of the mesosphere. This suggests, that the H_2O recycling at these pressure levels and chemical regimes is predominant and all broken down water is regenerated. Nevertheless, in the mesosphere at approx. 0.1 hPa, the effective yield decreases more strongly than the direct yield, reaching the minimum of 0.17 at 0.02 hPa, with a slight increase to 0.39 at the topmost layer at 0.01 hPa.
10 The value of 2 between 4 and 0.2 hPa reflects that all H from CH_4 reaches H_2O eventually at these altitudes, supporting the assumption as accepted in the literature. In the lower stratosphere and upper mesosphere, however, the box model results show that assuming a yield of 2 will lead to an overestimated H_2O production.

The yield of H_2 (see Fig. 3 (right)) shows a mostly anti-correlated behavior with respect to the yield of H_2O. Throughout most of the stratosphere the effective and direct yields of H_2 differ by about 0.2, while the effective yield drops down to
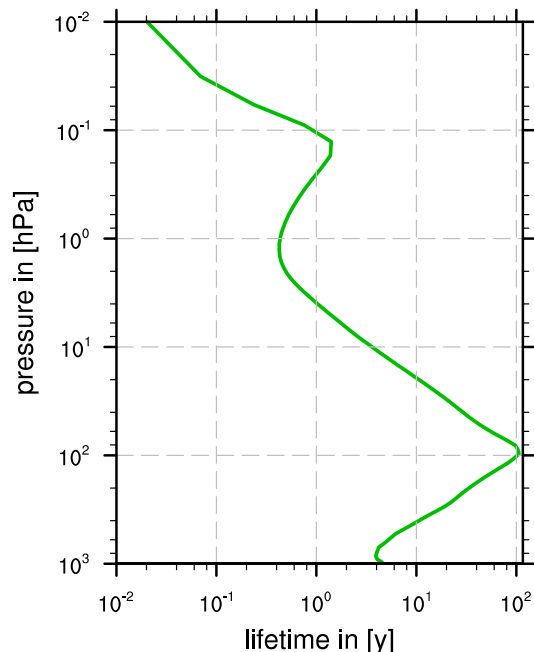
Figure 4. Vertical profile of CH_4 lifetime in the tropics with respect to removal by OH, $O(^1D)$, chlorine (Cl) and photolysis in years.

0 between 4 and 0.2 hPa, i.e. exactly in the region where the yield of H_2O attains its maximum. In accordance with the decreasing yield of H_2O, the direct and effective yields of H_2 increase substantially at higher altitudes, giving evidence that more and more H becomes diverted to and stays in H_2 instead of continuing towards H_2O.

A good indicator for the rate of general chemical reactivity in the atmosphere is the CH_4 lifetime, which is mostly influenced
5   by both, temperature, and the concentration of the reaction partners. The lifetime of CH_4 (τ_{CH_4}) with respect to its sinks OH, chlorine (Cl), $O(^1D)$ and photolysis is defined as:

$$\tau_{CH_4} = \frac{1}{(k_{OH} * [OH] + k_{Cl} * [Cl] + k_{O1D} * [O1D]) * c_{air} + j_{CH_4}} \tag{5}$$

with k_X being the reaction rate coefficients of CH_4+X in [cm3 s^{-1}], [X] being the mixing ratio of species X, c_{air} the concentration of dry air in [molecules cm^{-3}] and j_{CH_4} the photolysis rate of CH_4 in [molecules s^{-1}].

10   The area, where the H_2O yield attains its maximum, i.e. where it is 2, corresponds to the area, where the lifetime of CH_4 attains its stratospheric minimum (see Fig. 4). However, the CH_4 lifetime does not fully explain the behavior of the chemical yield, since in the upper mesosphere both, yield and lifetime, drop to a minimum, which can be explained by the emerging role of photolysis in this area. This further suggests that OH is an important factor in the H_2O yield in the stratosphere, but does not influence it alone. It becomes replaced by photolysis in the mesosphere, which influences the CH_4 lifetime and, more
15   importantly, destroys H_2O and initiates its recycling.

A sensitivity study concerning the impact of OH onto γ_{H_2O} is presented in the next section.

Table 2. Overview of simulations carried out in this study, including box model simulations and the sensitivity study concerning H_2O yield dependence on OH as well as the global simulations with EMAC.

Name	description	simulation
Exp1	Experiment with unconstrained OH	box model
Ref	Reference with standard fixed OH concentration from yearly climatology of RC1SD-base-10	box model
SS1	Sensitivity simulation with 0.5×OH from Ref	box model
SS2	Sensitivity simulation with 0.1×OH from Ref	box model
SS3	Sensitivity simulation with 0.05×OH from Ref	box model
SS4	Sensitivity simulation with 0.01×OH from Ref	box model
SS5	Sensitivity simulation with 2.0×OH from Ref	box model
Exp2	Global simulation with EMAC, MECCA and MECCA-TAG	CCM

3.1.2 Sensitivity with respect to OH

The results of the previous section reveal that the effective yield of water vapor from CH_4 oxidation depends on the box location, hence the chemical regime at a certain pressure level. Particularly, OH is one of the major oxidants shaping the chemical regime and largely controls the conversion of CH_4 to H_2 and H_2O , respectively. In the simulations shown above (Exp1) the OH is unconstrained, however, its final (equilibrated) OH concentration does not deviate much from the initial values (see Fig. 5). The following sensitivity study aims towards understanding the relationship between the OH and the vertical profile of the yield. It is investigated whether the variations of the yield are directly related to OH variations or to other parameters.

In further sensitivity simulations with CAABA, OH is initialized with the reference from EMAC multiplied with constants and kept constant throughout the simulation. This introduces an additional prescribed hydrogen carrying species, which introduces or withdraws hydrogen to or from the system. However, contribution of OH to the total H abundance in the system was found negligible. The first four simulations reduce the OH concentration by the factors of 0.5 (SS1), 0.1 (SS2), 0.05 (SS3) and 0.01 (SS4) respectively, while the fifth one is performed with a doubled OH concentration (SS5). One additional simulation represents the reference simulation (Ref), which started with an OH concentration identical to the analysis above, except that OH is kept constant. The simulations are listed in Table 2. The simulation set-up uses extreme perturbations of the OH concentration to provide a qualitative estimate of the impact of OH onto the H_2O yield from CH_4 oxidation.

The results of the sensitivity simulations are shown in Fig. 6. First of all, the initial experiment Exp1 (see Fig. 3) and the reference experiment of the sensitivity study Ref (see Fig. 6 red line), show mostly consistent results compared to each other concerning the effective and direct yield, which confirms that prescribing OH is adequate. However, in the upper mesosphere, where the OH concentration has the largest difference (cf. Fig. 5), the effective yield in the experiment Ref drops already at 1 hPa significantly. Additionally, the effective yield in the experiment Ref reaches a value lower than the effective yield in the
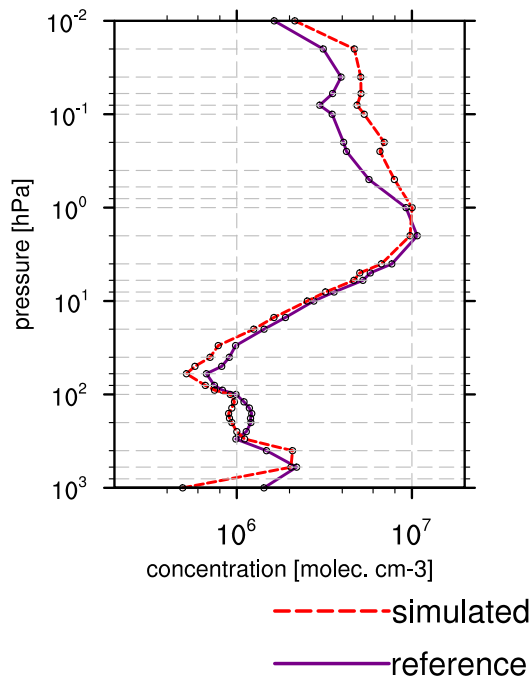
Figure 5. Reference OH concentration in the tropics from ESCiMo experiment RC1SD-base-10a (purple) and OH concentration as simulated in respective boxes (red).

experiment Exp1 in this area. Nevertheless, the direct yield is not considerably different between these two experiments. This once more supports the assumption of a strong OH dependence of the γ_{H_2O}.

Comparing experiment Ref with SS1 shows that reducing the OH concentrations by half reduces the direct and effective yields by about 0.05 in the lower stratosphere. Altogether, the direct yield profiles are rather similar in experiment Ref and SS1, with an exception of lower values in SS1 within the 10–1 hPa range and above 0.2 hPa. Prominent, however, is the difference in the effective yield. In the experiment SS1 the effective yield drops to zero already at 0.04 hPa and does not have the local enhancement seen in experiment Ref around 0.2–0.02 hPa.

Considering the sensitivity simulations SS2–SS4, the effect of OH reduction on γ_{H_2O} becomes more apparent. The effective yield drops to zero already above 60 hPa. The direct yield shows strongly reduced values in the stratosphere, with a local minimum at 20 hPa for SS2 and SS3 and a bit above for SS4, being 1.08, 0.92 and 0.78 respectively. Above 20 hPa the direct yield increases towards a local maximum at 2 hPa, following the profile of the CH_4 lifetime. Above 2 hPa the direct yield decreases nearly monotonically.

In the experiment SS5, with doubled OH, γ_{H_2O} is about 0.07 higher compared to experiment Ref and nearly replicates the results of experiment Exp1 in the mesosphere, where the OH equilibrated at a value of about twice that of the reference OH concentration from EMAC.
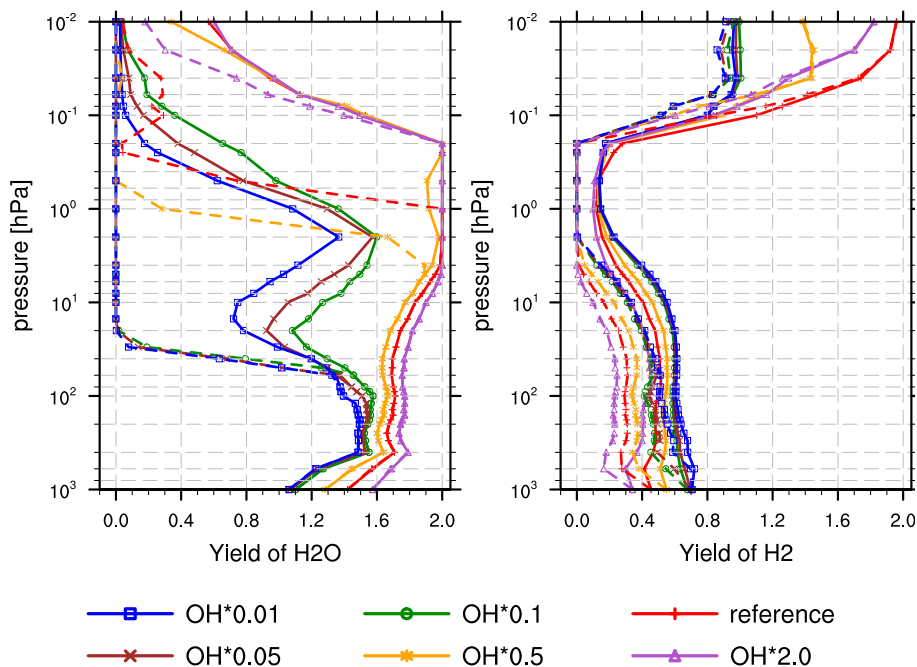
Figure 6. Pseudo vertical profiles of the H_2O yield (left) and H_2 yield (right), calculated by the box model approach. Solid lines represent the direct yield, the dashed lines the effective yield and circles indicate the pressure levels of the model boxes. OH concentrations are prescribed in all simulation to the initial values of the respective vertical box. The plot shows simulations with the reference OH concentration (Ref, red, plus signs) as well as the OH concentration times 2 (SS5, purple, triangles), times 0.5 (SS1, orange, asterisks), times 0.1 (SS2, green, circles), times 0.05 (SS3, brown, crosses) and times 0.01 (SS4, blue, squares).

Compared to the yields of H_2O, the effective and direct yields of H_2 show moderate dependence on OH concentration. The yield of H_2 is rather constant at lower levels, reaches its minimum around the stratopause and increases again above that to its maximum. Around the stratopause and in the lower mesosphere all experiments show similar results. In lower boxes the simulations with lower OH show higher yields and vice versa. In contrast to this, the boxes in the middle mesosphere and

5 above show an inverted behavior. Except, however, for experiment SS5, which results in a lower yield than in the reference simulation.

Moreover, profiles of yield of H_2 from the oxidation of CH_4 (γ_{H_2}) of experiments SS2, SS3 and SS4 overall do not vary much compared to each other.

Summarizing, increasing OH concentrations lead to higher direct and effective H_2O yields. Both yields show a larger differ-

10 ence to the reference at higher altitudes with varying OH, indicating that the sensitivity of the chemical regime with respect to the OH concentration increases with altitude.

The results of the sensitivity study suggest that the effective yield of H_2O has a high sensitivity to the OH concentration and give evidence that a minimum OH concentration is required for an effective H_2O recycling.
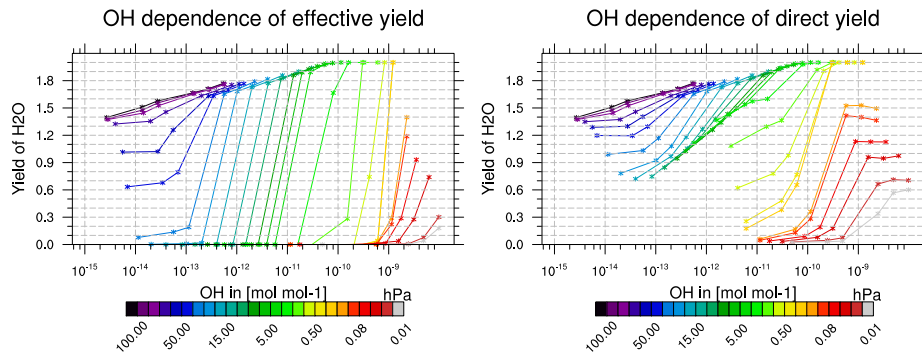
Figure 7. Effective yield (left) and direct yield (right) versus OH; colors indicate pressure level from low to high pressure.
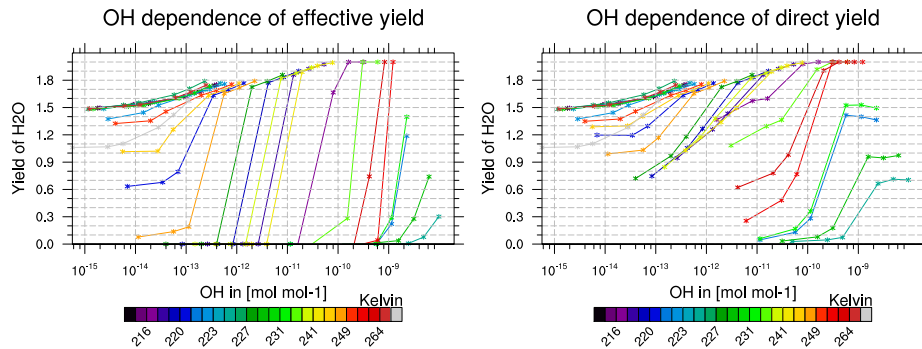
Figure 8. Effective yield (left) and direct yield (right) versus OH; colors indicate temperature from low to high temperature.

The γ_{H_2} shows an anti-correlated behavior to that of the H_2O yield, however, as an exception, doubling of OH shows a lower yield than the reference in the mesosphere.

3.1.3 Dependencies on pressure and temperature

The results shown in the previous subsection indicate that there is an OH dependence in both the effective and direct yield. To investigate whether this dependency is systematic, simulated H_2O yields are plotted as γ_{H_2O} versus OH mixing ratio in Fig. 7. Generally, there is no linear correlation between these two parameters. However, a systematic dependence is evident for each box, i.e. at each pressure level. The slope of the correlation is thereby dependent on the pressure level. For higher pressure the gradient is low and becomes steeper for lower pressure levels.

The slope of the correlation of OH and the direct yield (see Fig. 7 (right)) is smaller for pressure levels at 2–80 hPa than the slope of the effective yield (see Fig. 7 (left)) at corresponding pressure levels. Moreover, the effective yield has a sharp transition from low to high OH values, while the direct yield increases more gradually.

The scatter plots give evidence that in a certain range of pressure levels the yields exhibit a saturation-like behavior with respect to OH concentrations. Furthermore, there is no indication of a connection between the yield-OH-dependence and the
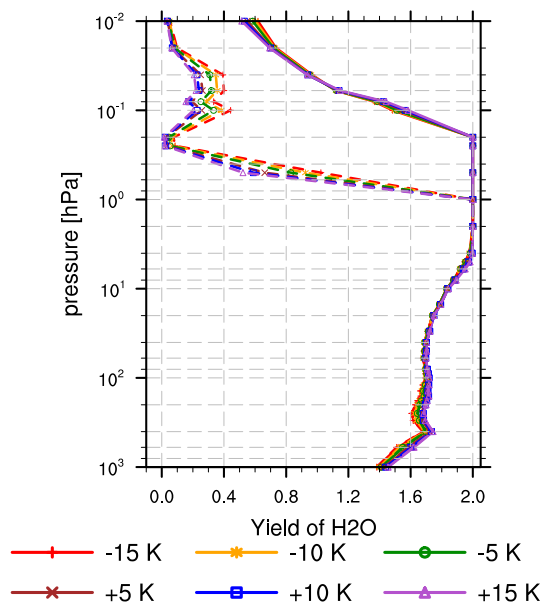
Figure 9. The pseudo vertical profile of the H_2O yield calculated by the box model approach. Solid lines represent the direct yield, the dashed lines the effective yield and circles indicate the pressure levels of the model boxes. OH is kept constant to the initial values of the respective vertical box. The plot shows sensitivities concerning temperature. Temperature is varied from the standard atmosphere value by -15K (red), -10K (orange), -5K (green), +5K (brown), +10K (blue) and +15 K (purple).

temperature (see Fig. 8 and the non-ordered colors indicating the temperature), despite the fact, that reaction rates in the $CH_4 \rightarrow H_2/H_2O$-cycle are usually stronger impacted by temperature than by pressure.

We carried out additional sensitivity studies in order to investigate the temperature dependence of the yield on a given pressure level. Results are displayed in Fig. 9. The simulation set-ups are identical to that of experiment Ref, except that 5 temperature in every box was varied within -15 K to +15 K with 5 K steps. This temperature range is chosen as it represents a range exceeding day-night differences (less than ± 5 K) and the annual cycle (less than ± 10 K) in the tropics. In the lower stratosphere there is no indication of a significant temperature sensitivity of the effective and direct yields. The latter also does not show any significant sensitivity at higher altitudes. The effective yield in the upper stratosphere and mesosphere shows a small dependence in a way that lower temperatures increase the yield and vice versa.

10 Consideration of the obvious vertical dependence and the very low temperature dependence gives evidence that not the physical parameters (temperature and pressure) themselves are crucial for the H_2O yield, but rather the chemical composition of the box (i.e., among others, abundances of OH, HO_2, $O(^1D)$ and Cl). This chemical composition, however, changes with altitude (hence with pressure) and depends additionally on transport.

3.2 Global model approach

As stated before, the box model approach does not take into account vertical transport and requires certain assumptions. Consequently, the boxes do not fully represent atmospheric conditions. To investigate the production of SWV in a comprehensive set-up, MECCA-TAG is applied in a global simulation with EMAC. The full chemistry of MECCA plus MECCA-TAG, which more than triples the amount of simulated tracers, increases the computational demands substantially. The additional tracers in the model defined by MECCA-TAG are basically counterparts of the tracers of the regular chemical mechanism and are marked (tagged) to be distinguishable from each other. In the following, these tracers are indicated by the label *tagged*. A spin-up simulation of 6 years with a reduced vertical resolution is carried out to pre-adjust tagged tracers. The results shown here originate from a subsequent simulation, which is executed for another two years model time.

Although the global simulation provides a three dimensional field, we focus in the current study on the vertical zonal mean profile of the yield of H_2O from CH_4 oxidation (γ_{H_2O}) averaged over the tropics. An analysis of the zonal mean without meridional averaging (see Supplement Fig. S1) shows that the conclusions presented in this section also apply to a certain degree at mid latitudes. In the polar regions the analysis of the calculated yield is not useful as long periods without sunlight and hence photolysis introduce substantial numerical errors into the calculation of γ_{H_2O}.

Figure 10 shows the vertical profile of the direct and effective yield of H_2O in the tropics (23° S–23° N). Both match the vertical profile of the results of the box model simulation Exp1 superficially. However, there are certain differences.

First, the yield of H_2O from CH_4 oxidation increases in the upper stratosphere and lower mesosphere to a value above 2, because the global model, unlike the box model, includes transport. The tagged intermediates (e.g. tagged CH_3, HCHO etc.) which are produced at lower levels are transported upward and are finally converted to H_2O. This results in a production of more than two H_2O molecules per oxidized CH_4 in one specific layer, because the additional production via transported intermediates is counted as well. In layers, where this increased production takes place, high OH concentration supports the conversion of the intermediates towards H_2O, since OH is the main driver of the chemistry.

The three topmost model layers in the upper mesosphere (0.06–0.01 hPa) are possibly subject to artifacts due to the nearby top of the global model and are therefore not considered in this analysis. It is assumed that the trend, which is evident below 0.1 hPa, showing decreasing γ_{H_2O} values also applies to the upper mesosphere, which would be similar to the box model results in the section above.

In Fig. 11 it also becomes obvious that the loss of H_2O increases at higher altitudes. Additionally, the recycling of H_2O contributes considerably to the effective yield. The photooxidation of H_2O drives the continuously recycling of H_2O to H_2 and back, shifting the equilibrium between these two gases towards H_2.

Altogether, the separated H_2O and H_2 loss/production terms of the global model are consistent with the box model findings. They also show a local maximum in loss of CH_4 and primary production of H_2O below the stratopause and the strongly pronounced secondary loss and production of H_2O in the middle and towards the upper mesosphere.
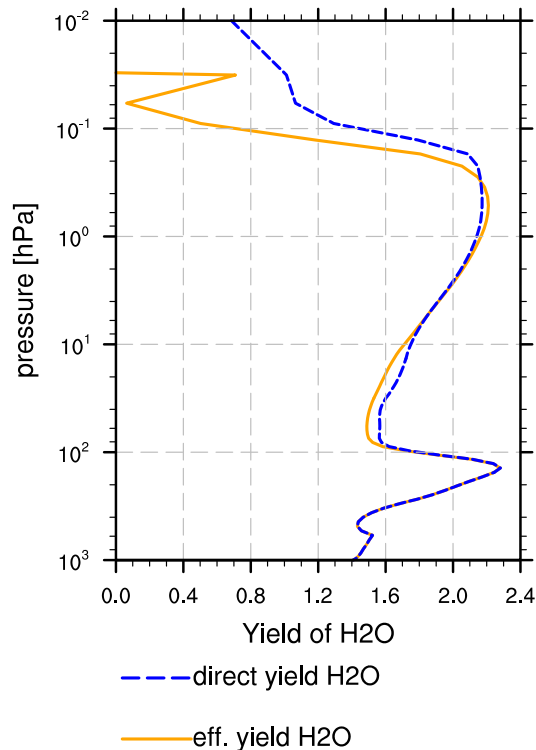
Figure 10. Effective and direct yield calculated from results of the global simulation in the tropics (23° S-23° N)

3.3 Ratio of H:H_2:H_2O

A different approach than the first two presented ones to determine γ_{H_2O} in the stratosphere is to use the fact that the vertical profile of the H content in terms of atoms is fairly constant above the tropopause (see Fig. 12) compared to tropospheric variations. The H content in the stratosphere consists mostly of CH_4, H_2O, H_2, and, in the topmost layers, H. Other H carrying substances, such as OH, HNO_3, can be neglected for the H budget. The chemical regime determines the proportion between H, H_2 and H_2O, but the total H content is preserved.

The effective yield of H_2O from CH_4 oxidation, as explained in previous sections, describes the net production of H_2O. Precisely it is an indicator for the interaction of loss and production of H_2O, further influencing the production of H_2 and H as well. As a first assumption, additional H from CH_4 oxidation should be partitioned to the reservoirs of H, H_2 and H_2O in the same proportion as is present in the steady state. This is based on the supposition that it does not matter, whether the H, which is injected to the hydrogen cycling and reaches the indicated H reservoirs, comes from CH_4 or any other hydrogen supply. If we assume further that the simulated proportion of H, H_2 and H_2O at a certain level is approximately constant in time and that CH_4 is at higher layers the only additional hydrogen supply, we can determine the effective yield of H_2O by CH_4
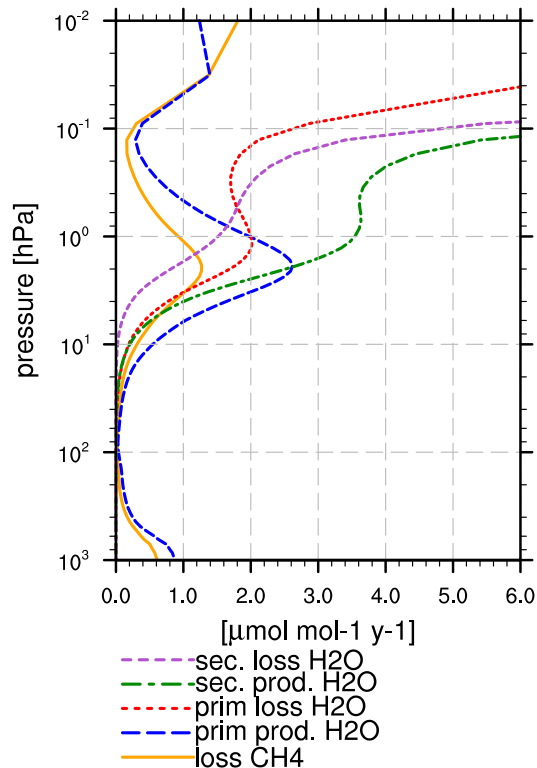
Figure 11. Separate loss of CH_4 and primary and secondary loss and production of H_2O from the global simulation (23° S-23° N).

oxidation through the proportion of H atoms in H_2O to the total hydrogen content of H, H_2 and H_2O. This proportion of the total hydrological content is subsequently called the H portion of H_2O.

In Fig. 13 the H portion of tagged and total H_2O is plotted with respect to the sum of tagged and total H in the CH_4 oxidation products H, H_2 and H_2O, from the global experiment Exp2. This sum (H + 2*H_2 + 2*H_2O + 4*CH_4) of 15 μmol mol^{-1} is in

5   accordance with the estimate derived with the CHEM2D model by Wrotny et al. (2010) for the sum of H_2 + H_2O + 2*CH_4 being $\sim$ 7.5 μmol mol^{-1} (i.e. one half of $\simeq$ 15 μmol mol^{-1}). The individual abundances of H_2, H_2O and CH_4 also agree well with each other.

The H portion of H_2O in the hydrogen budget is 2 in the troposphere and decreases to a minimum right above the tropopause. The hydrological cycle is producing a generally humid troposphere. Therefore, H_2O in the lower layers of the atmosphere is

10   prevailing versus H_2 and H, which are quickly oxidized as soon as they are produced. The minimum of the H portion of H_2O above the troposphere can be explained by the freeze drying at the cold point. This reduces the H portion of H_2O versus the one of H and H_2.

This minimum is not equally plain in the tagged H_2O. Note that tagged H_2O in the troposphere is already lower than the total H_2O, since it is solely produced by CH_4 oxidation. When CH_4 ascends from the troposphere through the cold point into
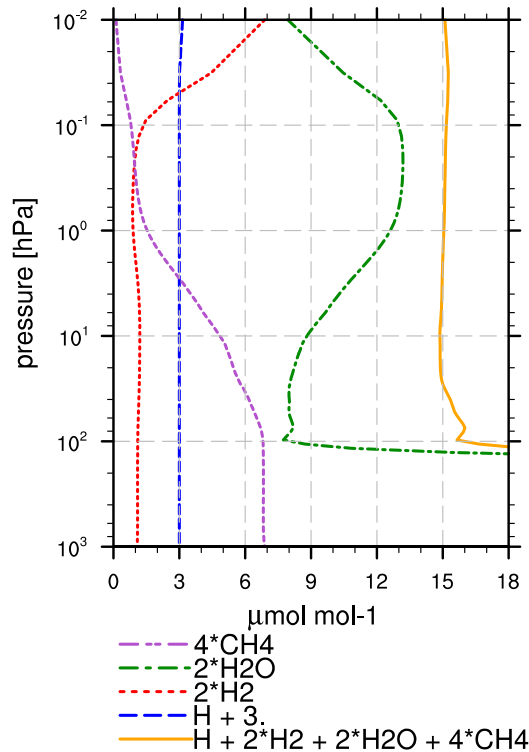
Figure 12. Annual zonal average of H content by species (in μmol mol^{-1}) over the tropics (23° S-23° N). H is shifted by 3.0 μmol mol^{-1} for a better visibility.

the stratosphere it continuously produces H_2O, although at low rates (due to low temperatures). Therefore, tagged H_2O is still produced by CH_4 and even though it partly freezes out, the proportion to H and H_2 is not much impacted. However, in the lower stratosphere the mixing ratio of tagged H_2 increases, while H_2O is still restrained by the cold point. This behavior becomes more apparent in case of the tagged species, since their absolute amounts are fairly low compared to the total ones.

5   Nevertheless, the H portion of tagged H_2O and total H_2O behave similar above the minimum at the tropopause, as seen in the maximum around the stratopause and in the lower mesosphere and the strong decrease in the middle mesosphere and above. The general behavior of the vertical profile also agrees well with the above findings of the yield calculations using box model and global model results.

4   Discussion

10   The presented results show three different approaches in estimating γ_{H_2O}. Taking the results of the separate approaches together gives the opportunity to discuss certain processes, which are differently parameterized and decisive for the yield estimation. We first want to discuss the general benefits and limitations of the approaches.
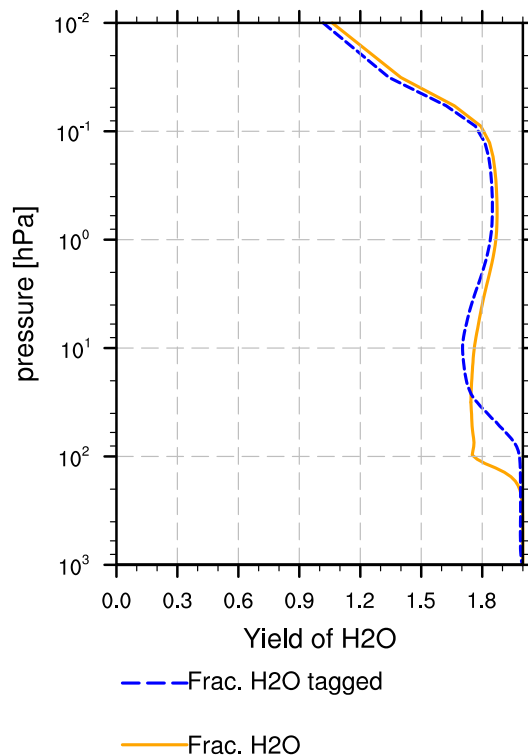
Figure 13. H portion of tagged and total H_2O with respect to the tagged and total hydrogen content (H+2×H_2+2×H_2O), respectively.

In the box model we have the opportunity to study a chemical regime without transport. It enables us to solely assess the involved chemical kinetics. Clearly, the box model chemistry does not fully represent the intended atmospheric conditions. Setting certain species to a constant value does change the chemical regime. However, without constraints on the chemical species the model would run into a new equilibrium, which changes the regime as well. It therefore needs careful weighing to specify, which species should be kept constant and which species should be allowed to re-adjust, to be able to simulate a representative chemical regime.

In the global model, we are not restricted to one vertical profile, but can evaluate the yield in three dimensions. Nevertheless, the effects of transport and chemical regime onto the yield cannot be separated, since transport influences the chemical regime. The vertical profile of γ_{H_2O} is for this reason susceptible to changes in dynamical processes as for example the Brewer-Dobson circulation.

The third approach, which used the total H budgets and portions, helps to quantitatively evaluate the methods, which are calculating the effective yield. It shows the actual portion of hydrogen from CH_4 in the total hydrogen without a production and loss term, which is sensitive to variations in the chemical regime. Yet, this approach is not directly linked to the loss of
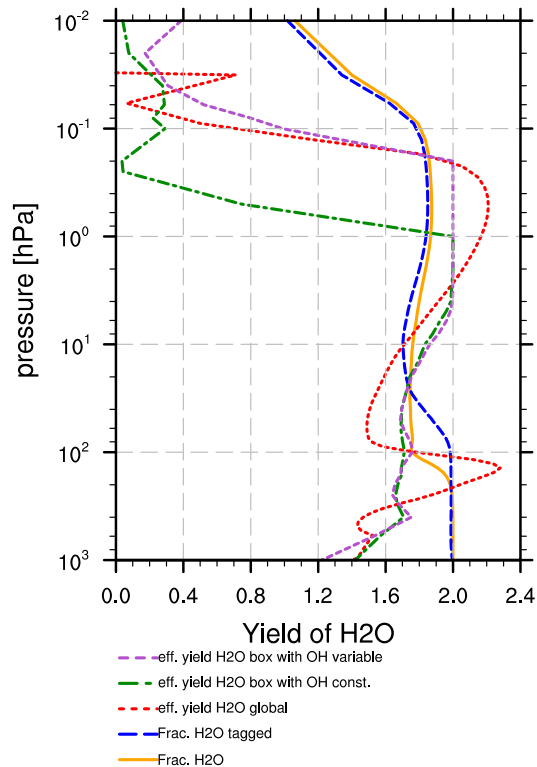
Figure 14. Comparison of all approaches determining the H_2O yield: Effective yield by box model simulations with variable OH (purple, dashed) and fixed OH (green, dash-dotted), effective yield by global model simulations (red, dotted), H portion of total (yellow, solid) and tagged (blue, long dashed) H_2O with respect to the hydrogen content.

CH_4 and it is not possible to explicitly resolve the influence of chemistry, since, for example, it is not clear if the decreasing values of γ_{H_2O} in the mesosphere are due to the increasing loss of H_2O or due to the reduced oxidation of CH_4.

Figure 14 shows the vertical profiles of the H_2O yields and H portions calculated by the approaches described in the previous sections combined in one plot.

Comparing the results of the box model and the global model in the lower stratosphere, γ_{H_2O} in the global model is lower than in the box model. This suggests that CH_4-produced H_2O is transported into the stratosphere, where it is destroyed, adding to the loss of H_2O. This reduces γ_{H_2O} while the oxidation of CH_4 is low, due to the exceptionally long lifetime of CH_4 due to low temperatures and low OH concentrations. In the upper stratosphere, global model γ_{H_2O} is larger than box model γ_{H_2O} and, more importantly, larger than 2, which is attributed to transport. This time, CH_4-derived intermediates are elevated and produce H_2O independent of the CH_4 oxidized in this region. This contradicts the assumption that two H_2O molecules are immediately produced from CH_4 oxidation, since intermediates do play an important role. This is furthermore consistent with the findings of Wrotny et al. (2010), who calculated a yield larger than 2 in this area as well.

In the middle mesosphere, box model and global model γ_{H_2O} decrease substantially. Although, the topmost layers must be considered with caution due to potential artifacts, it is possible that the yield of the global model reaches values below zero. In the global model tagged H_2O is transported into the mesosphere, where it is destroyed, due to the enhanced sink of H_2O through photooxidation. The effective yield decreases below zero, since the loss of H_2O becomes larger than the production of H_2O

5   ($\mathbf{P}^I_{H_2O} + \mathbf{P}^{II}_{H_2O} < \mathbf{L}^I_{H_2O} + \mathbf{L}^{II}_{H_2O}$). This emphasizes the importance of H_2O destruction at higher altitudes, which particularly is not included, when parameterizing the chemical γ_{H_2O} of H_2O with two H_2O molecules per CH_4 molecule oxidized.

Moreover, the effective yield in the box model setup with fixed OH profile drops down at 1 hPa, while the yield of the box model with variable OH, (Exp1) and the global model (Exp2) do not drop until 0.2 hPa. Additionally, Exp1 and Exp2 agree well concerning the altitude of the drop (the peak in Exp2 (red line) is most likely an artifact as discussed in Section 3.2). This

10   suggests further that the chemical regime of the box model presented by the annual mean of the reference simulation (Ref) is not consistent with the chemical regime at the corresponding altitude concerning OH. The initialized and fixed value of OH at these levels is too low to realistically capture the chemical situation. This also shows that unconstrained OH is crucial and that the vertical profile of OH of simulation Exp1 in this region better agrees with the OH in the global simulation Exp2.

The H portion of H_2O in the hydrogen content matches qualitatively the results of the yield calculations in the box and global

15   model approach. MECCA-TAG again enables us to focus on H in H_2O particularly from CH_4 oxidation and to ignore the H from other sources. The minimum of the H portion of H_2O in the lower stratosphere and its maximum close to the stratopause and in the lower mesosphere therefore shows that the production of H_2O from CH_4 oxidation relative to the production of H_2 from CH_4 oxidation is smaller in the lower stratosphere and becomes larger towards the upper stratosphere. Accordingly, we conclude that our estimation that γ_{H_2O} differs significantly from 2 in the lower stratosphere is reliable.

20   Altogether, the different approaches yield consistent results. All suggest a yield of less than 2 in the lower stratosphere, varying between 1.5 and 1.7. The smallest value is estimated in the global simulation Exp2, where the yield is larger than the one of le Texier et al. (1988), which is γ_{H_2O}=1.3 at corresponding altitudes. The results of le Texier et al. (1988) also showed a maximum around 1 hPa, which is consistent with our results, albeit being a bit above 1.8 and with that lower than our estimate of 2 (or more in case of the global simulation) in that region.

25   Overall, the estimated yield of H_2 from le Texier et al. (1988) and the yield of H_2 estimated by the box model approach are consistent as well. While our resulting γ_{H_2O} is larger than in le Texier et al. (1988), the γ_{H_2} is lower. Still, the vertical profiles of γ_{H_2} in both studies are comparable.

The fundamental study of le Texier et al. (1988) does not capture the influence of the increasing loss of H_2O at higher altitudes. They only considered the direct yield of H_2O and do not include H_2O loss in their calculation. Nevertheless, the

30   findings in our study show, that the difference between effective and direct yield becomes only apparent above 0.1 hPa and le Texier et al. (1988) do not discuss results above this pressure level.

Furthermore, le Texier et al. (1988) is often cited as the reference for the assumption of γ_{H_2O}=2. However, in the lower stratosphere our results and those of le Texier et al. (1988) actually agree that γ_{H_2O} is less than two, which objects the assumption of a constant γ_{H_2O}=2.

Hurst et al. (1999) calculated a net production of H_2O of 1.973 ± 0.003, which includes a loss of H via H_2 of 0.027 ± 0.003. These values differ from our findings in the box model approach. Our estimated γ_{H_2O} is smaller and our γ_{H_2} is larger than estimated by Hurst et al. (1999). As noted before, by using observational data it is not possible to distinguish between H_2 from the troposphere and H_2 produced by H from CH_4, which results in this rather low net production of H_2. Assume, for example,
5 that H_2 is not produced in the stratosphere. The mixing ratio of H_2 will then decrease with respect to altitude. However, the contribution from CH_4 oxidation onto H_2 fills up the oxidized molecules, and only if $\gamma_{H_2} \cdot [CH_4]$ is larger than the total loss of H_2, observed H_2 and CH_4 are anti-correlated. Using the kinetic tagging gives us the opportunity to distinguish between the total loss of H_2 and the loss of those H_2 molecules carrying H from CH_4. Our findings provide therefore an additional insight into processes, which determine the observed vertical profiles and provide estimates for the contribution of CH_4 separated from
10 the background H_2 and H_2O.

The study of Wrotny et al. (2010), based on a correlation analysis of satellite measurements, derived a yield of 2.6–2.7 at 1.0 hPa (depending on the satellite product and error assumptions). These are larger than our estimate, which is less than 2.3. Nevertheless, we agree that the yield can be larger than 2, but a direct comparison of our model results with the measurement based derivation of Wrotny et al. (2010) is not possible for the arguments given above.

15 Summarizing, our results suggest that applying γ_{H_2O}=2 as the contribution to H_2O by the oxidation of CH_4 in climate models likely overestimates the kinetic yield of H_2O in the lower stratosphere and in the mesosphere above 0.2 hPa. We admit, however, that a small fraction of H_2O should also be produced from H_2 ascending from the troposphere. This likely reduces the SWV bias in GCMs simulations using the approximation of γ_{H_2O}=2, since those models do not include a separate H_2O production from H_2 oxidation. Nevertheless, to be punctilious, the yield of H_2O from CH_4 oxidation should be distinguished
20 from the net chemical production of H_2O. In subsequent studies, we intend to apply the tagging method for estimating a γ_{H_2O} from H_2 oxidation ($\gamma_{H_2O}(H_2)$). H_2 and CH_4 may oxidize at a similar rate, but the resulting products are different, which likely results in a varied γ_{H_2O} with respect to the source gas (i.e. $\gamma_{H_2O}(CH_4) \neq \gamma_{H_2O}(H_2)$).

4.1 Recommendations for GCMs without on-line chemistry

An important disadvantage of the parameterization as in Eq. (1) with γ_{H_2O}=2 is that it does not account for the loss of H_2O
25 in the mesosphere. Even though CH_4 oxidation becomes negligible at these altitudes, this simple parameterization does not consider that H_2O gets chemically destroyed. Strictly speaking, the loss of H_2O is independent of CH_4 and should potentially be included separately. MacKenzie and Harwood (2004) and McCormack et al. (2008) presented, for example, sophisticated parameterizations, which target this issue in their 2D atmospheric models. Based on our results, we recommend to apply a parameterization, which is not solely based on the loss of CH_4, but accounts for the reduced yield in the lower stratosphere and
30 also includes the loss of H_2O.

Besides this, transport of intermediates is an important factor for the vertical profile of the γ_{H_2O}. It must be noted that atmospheric transport is not constant in time. The Brewer-Dobson circulation for example is predicted to change in future climate projections (Butchart et al., 2010). For a comprehensive parameterization of γ_{H_2O} these changes in transport must be taken into account. However, changes in transport depend on various factors and are therefore difficult to be included into

γ_{H_2O} parameterizations. This raises the question, whether a simplified parameterization of γ_{H_2O} is indeed applicable for future climate projections, or if it is necessary to simulate the full-chemistry for an accurate representation of SWV. The need of on-line chemistry for meaningful climate projections has anyway already been shown e.g. by Chiodo and Polvani (2017) for a realistic response of Southern Hemisphere (SH) circulation to CO_2 changes.

Nevertheless, one could start with a parameterization as introduced by Eq. (1), however, with a pressure dependent $\gamma_{H_2O}(p)$ derived from our vertical yield profiles. This adds a vertical dependency to the chemical production of H_2O per CH_4 oxidized. As long as no large variations or trends in the stratospheric transport are expected within the simulation period, our profile is a good approximation. The limitation is, however, that the pressure dependence is likely to change with changing climate.

At higher altitudes (above 0.2 hPa) the yield in Eq. (1) could be replaced or supplemented by an explicit parameterization of the chemical loss of H_2O, mostly via photolysis and the reaction with $O(^1D)$, see MacKenzie and Harwood (2004) and McCormack et al. (2008). In the simplified methane chemistry of EMAC, for example, a predefined $O(^1D)$ is also used for the reaction with CH_4 and could be reused for the reaction with H_2O. Again, the same limitation holds: under climate change, water vapour, and photolysis rates are likely to change.

5 Conclusions

In this study, we present a comprehensive evaluation of current assumptions and estimates of the chemical yield of H_2O from CH_4 oxidation in the middle atmosphere. We show results of three different approaches to estimate γ_{H_2O} and discuss certain advantages and challenges.

We conclude that the widely used assumption that one CH_4 molecule produces two water molecules overestimates the kinetic H_2O production in the stratosphere up to 4 hPa and in the mesosphere above 0.2 hPa. Our results show that a local yield larger than 2 in certain areas is possible through ascended intermediates. In addition to that, transport is generally an issue when dealing with kinetic yields, since it influences the chemical regimes at all altitudes. It also makes the interpretation of the presented approaches challenging, when these are investigated separately.

Nevertheless, the separate approaches presented in this study, show consistently that γ_{H_2O} is substantially lower than 2 in the lower stratosphere, has a local maximum between 0.2 and 0.4 hPa and is exceedingly low in the upper mesosphere. We find a low γ_{H_2O} in the middle and upper mesosphere, since the loss of H_2O at higher altitudes increases, shifting the equilibrium between H_2O and H_2 towards H_2. The chemical loss is therefore a crucial factor for the correct parameterization of SWV production from CH_4 oxidation. At some point, the loss of H_2O is so strong that H_2O is effectively destroyed per oxidized CH_4.

An additional result from the box model simulation is that the chemical yield of H_2O depends on the OH concentration and more general on the chemical kinetics. A strong temperature dependence, however, could not be detected.

Furthermore, the presented results agree with earlier kinetic estimates of γ_{H_2O} from le Texier et al. (1988), who state that not exactly two molecules are produced from CH_4 oxidation. Furthermore, our results give an additional insight into observations (e.g. Hurst et al. (1999); Rahn et al. (2003)), which are limited in detecting the chemical origin of H_2O.

Overall, the results of the separate approaches give evidence that calculating the yield of H_2O from CH_4 oxidation requires the loss of H_2O to be taken into account, making the task of creating a simple parameterization challenging. The latter also requires to admit a critical amount of assumptions about uncertain factors for an adequate atmospheric simulation. We therefore recommend, in order to maintain as much certainty as possible concerning the chemical yield of H_2O, to implement a simplified

5 H_2O chemistry including the most important reactions determining the H_2O yield. The extent of the resulting subset of the chemical mechanism is determinative for the correct representation of the H_2O content in the middle atmosphere. However, it must be noted that a set of reactions required for the comprehensive simulation of H_2O kinetics is not substantially different from the one incorporated in the full chemistry setup and is therefore less beneficial in terms of computational resources than a parameterized model. Nevertheless, as stated before, a too simple parameterization introduces uncertainties, which makes

10 it challenging to preserve the required accuracy for applications in the simulation of climate projections, where atmospheric dynamics (e.g. the Brewer-Dobson circulation) and chemistry potentially differ from the present-day atmosphere.

The investigations presented in this study should serve as a basis for future studies concerning the chemical yield of H_2O in the stratosphere and mesosphere. The gained knowledge can be used to derive new parameterizations of the chemical yield of H_2O for a potential application in GCMs.

15 *Code and data availability.* The Modular Earth Submodel System (MESSy) is continuously developed and applied by a consortium of institutions. The usage of MESSy and access to the source code is licensed to all affiliates of institutions, which are members of the MESSy Consortium. Institutions can become a member of the MESSy Consortium by signing the MESSy Memorandum of Understanding. More information can be found on the MESSy Consortium Web-site (http://www.messy-interface.org). The data of the box model simulations described above is available in the supplement. Data of the global simulation is available upon request from the corresponding author.

20 *Competing interests.* The authors declare that they have no conflict of interest.

Acknowledgements. We acknowledge the DLR internal project KliSAW (Klimarelevanz von atmosphärischen Spurengasen, Aerosolen und Wolken), which provided the financial basis for the presented study.

The model simulations have been performed at the German Climate Computing Centre (DKRZ) through support from the Bundesministerium für Bildung und Forschung (BMBF).

25 We used the NCAR Command Language (NCL) for data analysis and to create some of the figures of this study. NCL is developed by UCAR/NCAR/CISL/TDD and available on-line: http://dx.doi.org/10.5065/D6WD3XH5.

We furthermore thank all contributors of the project ESCiMo (Earth System Chemistry integrated Modelling), which provides the reference profiles and initial conditions as well as Christoph Kiemle for his internal review and valuable comments on the manuscript.

Supplement

- meccanism.pdf : The applied chemical mechanism of the box model and EMAC simulations.

- supplement.pdf : Including 2D Profiles of the EMAC simulations in terms of γ_{H_2O} and the ratio of H:H$_2$:H$_2$O, as well as the data of the box model simulations.

References

Austin, J., Wilson, J., Li, F., and Vömel, H.: Evolution of Water Vapor Concentrations and Stratospheric Age of Air in Coupled Chemistry-Climate Model Simulations, Am. Met. Soc., pp. 905–921, https://doi.org/10.1175/JAS3866.1, 2007.

Boville, B. A., Kiehl, J. T., Rasch, P. J., and Bryan, F. O.: Improvements to the NCAR CSM-1 for Transient Climate Simulations, J. Climate, 14, 164–179, https://doi.org/10.1175/1520-0442(2001)014<0164:ITTNCF>2.0.CO;2, 2001.

Butchart, N., Cionni, I., Eyring, V., Shepherd, T. G., Waugh, D. W., Akiyoshi, H., Austin, J., Brühl, C., Chipperfield, M. P., Cordero, E., Dameris, M., Deckert, R., Dhomse, S., Frith, S. M., Garcia, R. R., Gettelman, A., Giorgetta, M. A., Kinnison, D. E., Li, F., Mancini, E., McLandress, C., Pawson, S., Pitari, G., Plummer, D. A., Rozanov, E., Sassi, F., Scinocca, J. F., Shibata, K., Steil, B., and Tian, W.: Chemistry-Climate Model Simulations of Twenty-First Century Stratospheric Climate and Circulation Changes, J. Climate, 23, 5349–5374, https://doi.org/10.1175/2010JCLI3404.1, 2010.

Chiodo, G. and Polvani, L. M.: Reduced Southern Hemispheric circulation response to quadrupled CO_2 due to stratospheric ozone feedback, Geophys. Res. Lett., 44, 465–474, https://doi.org/10.1002/2016GL071011, 2017.

Dee, D. P., Uppala, S. M., Simmons, A. J., Berrisford, P., Poli, P., Kobayashi, S., Andrae, U., Balmaseda, M. A., Balsamo, G., Bauer, P., Bechtold, P., Beljaars, A. C. M., van de Berg, L., Bidlot, J., Bormann, N., Delsol, C., Dragani, R., Fuentes, M., Geer, A. J., Haimberger, L., Healy, S. B., Hersbach, H., Hólm, E. V., Isaksen, L., Kållberg, P., Köhler, M., Matricardi, M., McNally, A. P., Monge-Sanz, B. M., Morcrette, J.-J., Park, B.-K., Peubey, C., de Rosnay, P., Tavolato, C., Thépaut, J.-N., and Vitart, F.: The ERA-Interim reanalysis: configuration and performance of the data assimilation system, Quart. J. Roy. Meteor. Soc., 137, 553–597, https://doi.org/10.1002/qj.828, http://dx.doi.org/10.1002/qj.828, 2011.

Dessler, A. E., Weinstock, E. M., Hintsa, E. J., Anderson, J. G., Webster, C. R., May, R. D., Elkins, J. W., and Dutton, G. S.: An examination of the total hydrogen budget of the lower stratosphere, Geophys. Res. Lett., 21, 2563–2566, 1994.

digital dutch: https://www.digitaldutch.com/atmoscalc/, (last accessed Jan 2018), 1999.

ECMWF: IFS DOCUMENTATION - Cy31r1, Part IV: Physical Processes, https://www.ecmwf.int/sites/default/files/elibrary/2007/9221-part-iv-physical-processes.pdf, 2007.

Eichinger, R., Jöckel, P., Brinkop, S., Werner, M., and Lossow, S.: Simulation of the isotopic composition of stratospheric water vapour - Part 1: Description and evaluation of the EMAC model, Atmos. Chem. Phys., 15, 5537–5555, https://doi.org/10.5194/acp-15-5537-2015, 2015.

Forster, P. M. d. F. and Shine, K. P.: Stratospheric water vapour changes as a possible contributor to observed stratospheric cooling, Geophys. Res. Lett., 26, 3309–3312, https://doi.org/10.1029/1999GL010487, 1999.

Fueglistaler, S. and Haynes, P. H.: Control of interannual and longer-term variability of stratospheric water vapor, J. Geophys. Res., 110, D24 108, https://doi.org/https://doi.org/10.1029/2005JD006019, 2005.

Gromov, S., Jöckel, P., Sander, R., and Brenninkmeijer, C. A. M.: A kinetic chemistry tagging technique and its application to modelling the stable isotopic composition of atmospheric trace gases, Geosci. Model Dev., 3, 337–364, https://doi.org/10.5194/gmd-3-337-2010, www.geosci-model-dev.net/3/337/2010/, 2010.

Hurst, D., Dutton, G., Romashkin, P., Wamsley, P., Moore, F., Elkins, J., Hintsa, E., Weinstock, E., Herman, R., Moyer, E., Scott, D., May, R., and Webster, C.: Closure of the total hydrogen budget of the northern extratropical lower stratosphere, J. Geophys. Res. Atmos., 104, 8191–8200, 1999.

IPCC: Climate Change 2013: The Physical Science Basis. Contribution of Working Group I to the Fifth Assessment Report of the Intergovernmental Panel on Climate Change, Cambridge University Press, Cambridge, United Kingdom and New York, NY, USA, https://doi.org/10.1017/CBO9781107415324, www.climatechange2013.org, 2013.

Jöckel, P., Kerkweg, A., Pozzer, A., Sander, R., Tost, H., Riede, H., Baumgaertner, A., Gromov, S., and Kern, B.: Development cycle 2 of the Modular Earth Submodel System MESSy2, Geosci. Model Dev., 3, 717–752, https://doi.org/10.5194/gmd-3-717-2010, manual, 2010.

Jöckel, P., Tost, H., Pozzer, A., Kunze, M., Kirner, O., Brenninkmeijer, C. A. M., Brinkop, S., Cai, D. S., Dyroff, C., Eckstein, J., Frank, F., Garny, H., Gottschaldt, K.-D., Graf, P., Grewe, V., , Kerkweg, A., Kern, B., Matthes, S., Mertens, M., Meul, S., Neumaier, M., Nützel, M., Oberländer-Hayn, S., Ruhnke, R., Runde, T., Sander, R., Scharffe, D., and Zahn, A.: Earth System Chemistry integrated Modelling (ESCiMo) with the Modular Earth Submodel System (MESSy) version 2.51, Geosci. Model Dev., 9, 1153–1200, https://doi.org/10.5194/gmd-9-1153-2016, http://www.geosci-model-dev.net/9/1153/2016/gmd-9-1153-2016.html, 2016.

Johnston, H. and Kinnison, D.: Methane photooxidation in the atmosphere: Contrast between two methods of analysis, J. Geophys. Res., 103, 21 967–21 984, 1998.

le Texier, H., Solomon, S., and Garcia, R. R.: The role of molecular hydrogen and methane oxidation in the water vapour budget of the stratosphere, Quart. J. Roy. Meteor. Soc., 114, 281–295, https://doi.org/10.1002/qj.49711448002, 1988.

Lehmann, R.: An Algorithm for the Determination of All Significant Pathways in Chemical Reaction Systems, J. Atmos. Chem., 47, 45–78, https://doi.org/10.1023/B:JOCH.0000012284.28801.b1, 2004.

MacKenzie, I. A. and Harwood, R. S.: Middle-atmospheric response to a future increase in humidity arising from increased methane abundance, J. Geophys. Res., 109, D02 107, https://doi.org/10.1029/2003JD003590, 2004.

Maycock, A. C., Joshi, J. M., Shine, K. P., Davis, S. M., and Rosenlof, K. H.: The potential impact of changes in lower stratospheric water vapour on stratospheric temperatures over the past 30 years, Quart. J. Roy. Meteor. Soc., 26, 2176–2185, https://doi.org/10.1002/qj.2287, 2014.

McCormack, J. P., Hoppel, K. W., and Siskind, D. E.: Parameterization of middle atmospheric water vapor photochemistry for high-altitude NWP and data assimilation, Atmos. Chem. Phys., 8, 7519–7532, https://doi.org/10.5194/acp-8-7519-2008, https://www.atmos-chem-phys.net/8/7519/2008, 2008.

Monge-Sanz, B. M., Chipperfield, M. P., Untch, A., Morcrette, J.-J., Rap, A., and Simmons, A. J.: On the uses of a new linear scheme for stratospheric methane in global models: water source, transport tracer and radiative forcing, Atmos. Chem. Phys., 13, 9641–9660, https://doi.org/10.5194/acp-13-9641-2013, https://www.atmos-chem-phys.net/13/9641/2013/, 2013.

Mote, P.: The annual cycle of stratospheric water vapor in a general circulation model, J. Geophys. Res., 100, 7363–7379, https://doi.org/10.1029/94JD03301, http://onlinelibrary.wiley.com/doi/10.1029/94JD03301/pdf, 1995.

Myhre, G., Nilsen, J. S., Gulstad, L., Shine, K. P., Rognerud, B., and Isaksen, I. S. A.: Radiative forcing due to stratospheric water vapour from CH_4 oxidation, Geophys. Res. Lett., 34, L01 807, https://doi.org/10.1029/2006GL027472, 2007.

NOAA/NASA: U.S. Standard Atmosphere 1976 (NASA-TM-X-74335), National Oceanic and Atmospheric Administration / National Aeronautics and Space Administration, 1976.

Oman, L., Waugh, D. W., Pawson, S., Stolarski, R. S., and Nielsen, J. E.: Understanding the Changes of Stratospheric Water Vapor in Coupled Chemistry–Climate Model Simulations, J. Atmos. Sci., 65, 3278–3291, https://doi.org/10.1175/2008JAS2696.1, 2008.

Rahn, T., Eiler, J. M., Boering, K. a., Wennberg, P. O., McCarthy, M. C., Tyler, S., Schauffler, S., Donnelly, S., and Atlas, E.: Extreme deuterium enrichment in stratospheric hydrogen and the global atmospheric budget of H_2., Nature, 424, 918–921, https://doi.org/10.1038/nature01917, 2003.

Revell, L., Stenke, A., Rozanov, E., Ball, W., Lossow, S., and Peter, T.: The role of methane in projections of 21st century stratospheric water vapour, Atmos. Chem. Phys., 16, 13 067–13 080, https://doi.org/10.5194/acp-16-13067-2016, www.atmos-chem-phys.net/16/13067/2016/, 2016.

Revell, L. E., Bodeker, G. E., Huck, P. E., Williamson, B. E., , and Rozanov, E.: The sensitivity of stratospheric ozone changes through the 21st century to N_2O and CH_4, Atmos. Chem. Phys., 12, 11 309–11 317, https://doi.org/10.5194/acp-12-11309-2012, www.atmos-chem-phys.net/12/11309/2012/, 2012.

Roeckner, E., Brokopf, R., Esch, M., Giorgetta, M., Hagemann, S., Kornblueh, L., Manzini, E., Schlese, U., and Schulzweida, U.: Sensitivity of Simulated Climate to Horizontal and Vertical Resolution in the ECHAM5 Atmosphere Model, American Meterological Society, 19, 3771–3791, 2006.

Rohs, S., Schiller, C., Riese, M., Engel, A., Schmidt, U., Wetter, T., Levin, I., Nakazawa, T., and Aoki, S.: Long-term changes of methane and hydrogen in the stratosphere in the period 1978-2003 and their impact on the abundance of stratospheric water vapor, J. Geophys. Res. Atmos., 111, 1–12, https://doi.org/10.1029/2005JD006877, 2006.

Sander, R., Kerkweg, A., Jöckel, P., and Lelieveld, J.: Technical note: The new comprehensive atmospheric chemistry module MECCA, Atmos. Chem. Phys., 5, 445–450, 2005.

Sander, R., Baumgaertner, A., Gromov, S., Harder, H., Jöckel, P., Kerkweg, A., Kubistin, D., Regelin, E., Riede, H., Sandu, A., Taraborrelli, D., Tost, H., and Xie, Z.-Q.: The atmospheric chemistry box model CAABA/MECCA-3.0, Geosci. Model Dev., 4, 373–380, https://doi.org/10.5194/gmd-4-373-2011, 2011a.

Sander, R., Jöckel, P., Kirner, O., Kunert, A. T., Landgraf, J., and Pozzer, A.: The photolysis module JVAL-14, compatible with the MESSy standard, and the JVal PreProcessor (JVPP), Geosci. Model Dev., 7, 2653–2662, https://doi.org/10.5194/gmd-7-2653-2014, www.geosci-model-dev.net/7/2653/2014/, 2014.

Sander, S. P., Abbatt, J., Barker, J. R., Burkholder, J. B., Friedl, R. R., Golden, D. M., Huie, R. E., Kolb, C. E., Kurylo, M. J., Moortgat, G. K., Orkin, V. L., and Wine, P. H.: Chemical Kinetics and Photochemical Data for Use in Atmospheric Studies, Evaluation No. 17, JPL Publication 10-6, Jet Propulsion Laboratory, https://doi.org/10.1002/kin.550171010, http://jpldataeval.jpl.nasa.gov/, 2011b.

Solomon, S., Rosenlof, K. H., Portmann, R. W., Daniel, J. S., Davis, S. M., Sanford, T. J., and Plattner, G.-K.: Contributions of Stratospheric Water Vapor to Decadal Changes in the Rate of Global Warming, Science, 327, 1219–1223, https://doi.org/10.1126/science.1182488, 2010.

Stenke, A. and Grewe, V.: Simulation of stratospheric water vapor trends: impact on stratospheric ozone chemistry, Atmos. Chem. Phys., 5, 1257–1272, www.atmos-chem-phys.org/acp/5/1257/, 2005.

Stowasser, M., Oelhaf, H., Wetzel, G., Friedl-Vallon, F., Maucher, G., Seefeldner, M., Trieschmann, O., v. Clarmann, T., and Fischer, H.: Simultaneous measurements of HDO, H_2O, and CH_4 with MIPAS-B: Hydrogen budget and indication of dehydration inside the polar vortex, J. Geophys. Res., 104, 19 213–19 225, 1999.

Wrotny, J. E., Nedoluha, G. E., Boone, C., Stiller, G. P., and McCormack, J. P.: Total hydrogen budget of the equatorial upper stratosphere, Journal of Geophysical Research: Atmospheres, 115, https://doi.org/10.1029/2009JD012135, https://agupubs.onlinelibrary.wiley.com/doi/abs/10.1029/2009JD012135, 2010.

<